

# Effects of Processing on Microstructure and Mechanical Properties of Ti-6Al-4V Fabricated using Electron Beam Melting (EBM): Orientation and Location \*

Nikolas Hrabe<sup>a</sup>, Ryan Kircher<sup>b</sup>, Timothy Quinn<sup>a</sup>

<sup>a</sup>National Institute of Standards and Technology (NIST), Boulder, CO

<sup>b</sup>Medical Modeling Inc., Golden, CO

\* Official contribution of the National Institute of Standards and Technology; not subject to copyright in the United States.

## ABSTRACT

Electron beam melted (EBM) titanium alloy (Ti-6Al-4V) samples were built and characterized (qualitative prior- $\beta$  grain size, quantitative  $\alpha$  lath thickness, monotonic tensile, Vickers microhardness) to determine the effect of location and orientation on microstructure and properties. Samples of vertical orientation, compared to horizontal, were found to have 30% lower elongation. Orientation within the x-y plane as well as location were found to have less than 3 % effect on mechanical properties, and it is possible a second order effect of thermal mass contributed to these results.

## INTRODUCTION

Processing variables for selective electron beam melting (EBM) can be divided into two main categories: inter-build and intra-build. Inter-build variations occur across multiple builds, whereas intra-build variations occur within one build space and potentially within one part. For EBM as well as other additive manufacturing techniques it is important to understand the effects both types of these variables have on microstructure and properties in order to achieve material of acceptable quality, repeatability, and reproducibility. Examples of inter-build processing variables that have been investigated previously are chemistry (both starting powder and as-built material) [1] and build plate temperature [2].

The present work focuses on intra-build variations and specifically location and orientation. For location we hypothesized that relative temperature would decrease radially outward to the exterior of the build space, and it was expected that as relative temperature decreased, cooling rate and time above  $\beta$  transus would increase. For the expected Ti-6Al-4V microstructure (known as acicular, lamellar, or Widmanstätten), as cooling rate decreases,  $\alpha$  lath thickness is known to increase, leading to lower ultimate tensile strength (UTS), yield strength (YS), and microhardness [3-9]. Another microstructural feature characterized in this work, prior- $\beta$  grain size, is controlled by time above the  $\beta$  transus. For the expected Ti-6Al-4V microstructure, as time above the  $\beta$  transus increases, prior- $\beta$  grain size increases, leading to lower UTS, YS, and microhardness [3-9]. Considering the known microstructure-mechanical property relationships for the expected Ti-6Al-4V microstructure, it was expected that exterior parts would have finer microstructure (both  $\alpha$  laths and prior- $\beta$  grains) and higher mechanical properties (UTS, YS, microhardness) compared to parts on the interior. The part geometry

developed for this work provides the opportunity to isolate the location variable, and to the knowledge of the authors, this has not been done previously.

Orientation was the second intra-build variable investigated, and two separate comparisons were made: horizontally oriented vs. vertically oriented as well as x-oriented vs. y-oriented parts. For EBM processed Ti-6Al-4V, elongated prior- $\beta$  grains and microstructural texture has been previously observed in the z-direction [2], and it was expected that these factors would be the dominant mechanism responsible for any observed effects of orientation. Horizontally oriented and vertically oriented parts have been compared previously, including two studies on EBM processed Ti-6Al-4V. The first [10] reported no difference in UTS or YS, and the horizontal part displayed higher percent elongation at break (% EL). The second reported no difference in YS, but UTS was higher and % EL lower for the horizontal part [11]. There was not enough part layout information provided in the second study to speculate on reasons for the difference in trends. Classically annealed bulk Ti-6Al-4V, of the same microstructure as that expected for EBM Ti-6Al-4V, has previously been reported to exhibit increasing % EL with decreasing prior- $\beta$  grain size [5, 6]. The mechanism reported was reduced slip length for the shorter prior- $\beta$  grain boundary lengths of smaller prior- $\beta$  grains lead to shorter dislocation pile-up lengths, reduced stress concentrations at triple-point grain boundary intersections, delayed crack initiation, and increased % EL. Considering these bulk material results and the elongated prior- $\beta$  grain morphology in the z-direction for EBM Ti-6Al-4V [2], horizontally oriented parts were expected to have higher % EL compared to vertically oriented parts because horizontally oriented parts would have shorter prior- $\beta$  grain boundary lengths in the tensile loading axis. In [12] tensile data was collected for Ti-6Al-4V fabricated using electron beam freeform fabrication (EBF<sup>3</sup>), a process similar to EBM. No intra-build comparison to work presented here can be made because all the specimens were taken from the same part, and the heat transfer dynamics of the wire fed EBF<sup>3</sup> differ from that of the powder bed process of EBM.

Orientation effects within the x-y plane were also investigated in this work, and as the tensile axes were all orthogonal to the elongated prior- $\beta$  grain and microstructural texture direction, we expected no difference would be observed in microstructure or mechanical properties.

## **MATERIALS AND METHODS**

All parts were built in one batch, and the position and orientation of each part in the 200 mm x 200 mm build space (centered on the 210 mm x 210 mm build plate) was chosen to isolate each intra-batch variable and minimize effects from other variables (Figure 1). Tensile, microstructure, and microhardness specimens were cut from the as-built parts and prepared for testing. After testing, results were analyzed to determine any variation in microstructure or mechanical properties as a function of energy input, orientation, and location.

Arcam S12 EBM equipment<sup>1</sup> (software version 3.2.45.12281, accelerating voltage 60 kV, layer thickness 70  $\mu\text{m}$ , “standard” Arcam build theme for Ti-6Al-4V) was used with gas atomized Ti-6Al-4V powder (average particle size 70  $\mu\text{m}$ ). This build theme varies electron beam parameters in a controlled sequence throughout the build according to algorithms developed by the manufacturer in an effort to achieve fully dense as-built parts with consistent

microstructure and properties. Part 1 was built with a speed factor of 30. Parts 2-6 were built with a speed factor of 40. This range of speed factor represents the limits within which complete melting and fully dense as-built parts can be expected. Speed factor is a manufacturer-specific variable that describes the more generic electron beam parameters such as beam current and beam speed as they relate to a given manufacturer-specific build theme. Therefore, specific values of beam current and beam speed cannot be known from the speed factor because they are constantly being varied by the build theme throughout the build. Since speed factor has little practical use for additive manufacturing systems other than the one used in this work, it should be thought of in terms of its inverse relationship with energy input.

Adjacent parts had 1 mm space between them, which was assumed to be enough space to thermally isolate each part. The dimensions of horizontally built parts 1, 2, and 4 were the same (x-dimension 159 mm, y-dimension 14 mm, and z-dimension 27 mm). Horizontally built part 6 had the same dimensions but a different orientation (x-dimension 14 mm, y-dimension 159 mm, and z-dimension 27 mm). Parts 3 and 5 also had the same dimensions but were built in the vertical orientation (x-dimension 27 mm, y-dimension 14 mm, and z-dimension 159 mm).

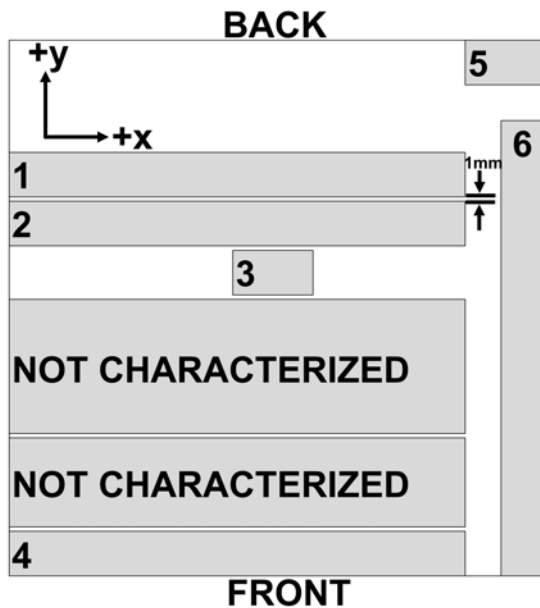


Figure 1. Top view schematic of part layout/orientation in 200 mm x 200 mm build space. A 1 mm spacing was used between adjacent parts.

Chemistry was measured for the as-built parts and compared to *ASTM F2924 Standard Specification for Additive Manufacturing Titanium-6 Aluminum-4 Vanadium with Powder Bed Fusion*. Aluminum, vanadium, and iron were measured by optical emission spectroscopy (OES). Oxygen, nitrogen, and hydrogen were measured by inert gas fusion. Carbon was measured by the combustion method. Approximate uncertainties in each measurement were as follows: oxygen (3 %), nitrogen (14 %), hydrogen (6 %), and carbon (6 %). Uncertainties for aluminum, vanadium, and iron were not available.

Bulk tensile samples (Figure 2b) were cut from as-built parts (Figure 2a) by use of electric discharge machining (EDM). Each tensile sample was sliced by use of EDM into ten thin

tensile specimens (Figure 2c) used for monotonic tensile testing. Results from previous work by this author [13] showed negligible variation of microstructure and properties within a given part as a function of distance from the build plate. Therefore, for each part, mechanical properties will be reported as an average of the values for each of the 10 tensile specimen slices. Tensile specimens were approximately equal to the rectangular cross-section subsize specimens of *ASTM E8 Standard Test Methods for Tension Testing of Metallic Materials* with the following gauge dimensions: length 25 mm, width 5 mm, and thickness 2 mm ( $\pm 0.1$  mm tolerance for all dimensions). By use of the orientation nomenclature from *ASTM 2921 Standard Terminology for Additive Manufacturing – Coordinate Systems and Test Methodology*, tensile specimens for each part had the following orientation: parts 1, 2, and 4 – XY; parts 3 and 5 – ZY; part 6 – YX. The remaining material after cutting the bulk tensile sample (Figure 2d) was sectioned for metallographic mounting (Figure 2e), and the same piece was used to characterize microhardness and microstructure. It is important to note that this microhardness/microstructure piece is directly adjacent to the tensile specimen gauge sections, allowing appropriate comparisons between microstructure, microhardness, and mechanical properties. Nonparametric ANOVA (Kruskal-Wallis) statistical analysis was performed for comparisons between parts or between distances from the build plate within a given part. P-values less than 0.05 were considered significant.

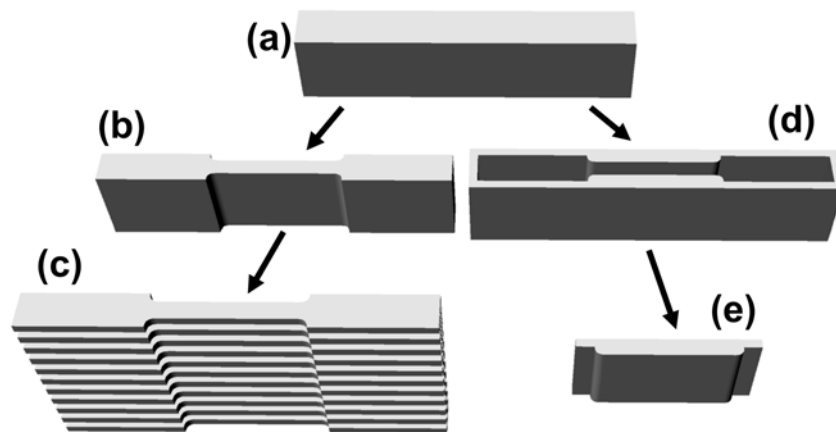
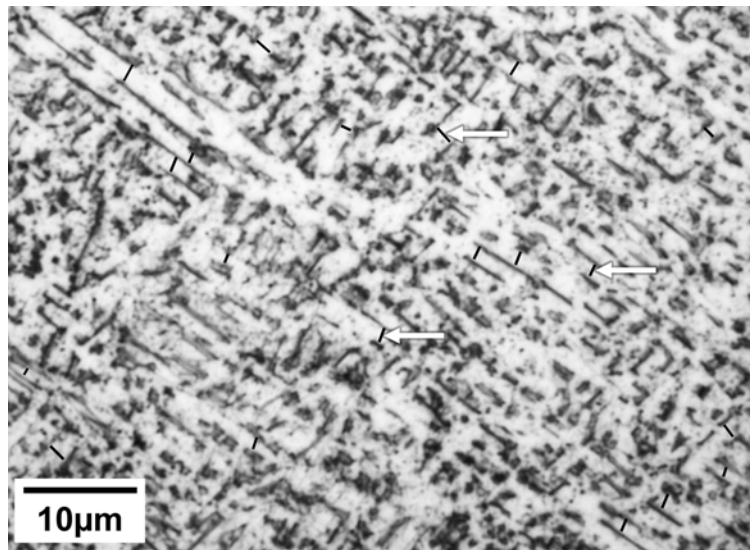


Figure 2. (a) as-built part, (b) bulk tensile sample cut from as-built part, (c) tensile specimens after slicing tensile sample, (d) remnant after cutting bulk tensile sample, (e) smaller piece cut from remnant used for microhardness and microstructure characterization. All cutting operations performed by use of EDM.

Monotonic tensile testing was performed according to ASTM E8 for all specimens at a strain rate of  $10^{-3} \text{ sec}^{-1}$ . Yield strength (YS, 0.2 % offset method), elongation at break (% EL), and ultimate tensile strength (UTS) were measured from the engineering stress-strain curve of each specimen. Tensile specimen fracture surfaces were observed using scanning electron microscopy (SEM). The microstructure/microhardness piece of each part (Figure 2e) was mounted and polished to a  $0.02 \mu\text{m}$  finish after removal of EDM layer. Ten Vickers microhardness measurements (1000gf, 55x, 20 second hold,  $>2.5$  indentation width spacing between adjacent indentations) were taken at distances equivalent to the middle of each of the 10 tensile specimens for a total of 100 indentations per part. Microstructure/microhardness pieces were then etched (Kroll's etchant) and both prior- $\beta$  grain size as well as  $\alpha$  lath thickness were

observed under an optical microscope. For the expected Ti-6Al-4V microstructure, prior- $\beta$  grain size increases with increasing time above the  $\beta$  transus, leading to lower UTS, YS, and microhardness [3-9]. This microstructural feature was qualitatively assessed by use of lower magnification images taken under low-angle light. This light was necessary to achieve sufficient contrast between grains, but it also resulted in inconsistent lighting, leaving the top of most images darker than the bottom. It is important to note that this gradient of brightness is only due to the low-angle light and should not be mistaken as a microstructural feature. Quantitative measurements were not possible due to lack of grain boundary definition ( $\alpha$  did not segregate to all grain boundaries).  $\alpha$  lath thickness was quantified with the use of Image J<sup>1</sup> [14] and higher magnification optical microscope images (Figure 3). Three images were taken adjacent to the microhardness indentations for each represented tensile specimen, and 20  $\alpha$  laths were measured for each image totalling 600  $\alpha$  laths measured for each part. It is important to note that the quantification method chosen depends on the subjective judgment of the person making the measurement, and any potential measurement errors were minimized by having a single person make all measurements.



*Figure 3. Representative high magnification optical microscope image of EBM Ti-6Al-4V microstructure (light phase =  $\alpha$ , dark phase =  $\beta$ ), including measurements of  $\alpha$  lath thickness (black lines, some denoted by white arrows). The lines were drawn by the operator, and Image J automatically recorded their length.*

## RESULTS

### Microstructure

The microstructure of EBM processed Ti-6AL-4V (Figure 3) observed in this work is similar to other EBM Ti-6Al-4V [11] but differs slightly from the expected acicular or Widmanstätten microstructure obtained through classical annealing [8]. The classical morphology is discrete  $\alpha$  in continuous  $\beta$ , but in the EBM microstructure of this work it appears  $\alpha$  is continuous and  $\beta$  is discrete.

## Chemistry

Chemistry is reported to help understand the observed magnitudes of mechanical properties. The measured chemistry of as-built parts (Table I) met ASTM F1472, except for oxygen. Out-of-specification oxygen content in as-built parts is due to out-of-specification oxygen in the powder (0.21 wt %). Failure of any parts in this study to meet mechanical property requirements might be attributed to high oxygen content. Out-of-specification oxygen was acceptable for this work because parts within the same build were compared, and if it is assumed chemistry does not change within a build, then any effects of intra-build processing variables could still be observed.

*Table I. Measured as-built part chemistry (in wt %) was out-of-specification for oxygen compared to additive manufactured Ti-6Al-4V with powder bed fusion. Measurement uncertainties for iron, aluminum, and vanadium were not available. Out-of-specification oxygen content in as-built parts is from out-of-specification oxygen content in powder (0.21 wt %).*

	<b>N</b>	<b>C</b>	<b>H</b>	<b>Fe</b>	<b>O</b>	<b>Al</b>	<b>V</b>
ASTM F2924	0.05 max	0.10 max	0.015 max	0.30 max	0.20 max	5.5-6.75	3.5-4.5
as-built	0.031±0.004	0.019±0.001	0.0008±0.00005	0.2	0.22±0.007	6.1	4.07

## Location – horizontal

We hypothesized that the exterior of the build space might be cooler and lead to higher cooling rates than the interior of the build space. Therefore, it was expected that compared to interior part 2, exterior part 4 would exhibit finer  $\alpha$  laths and higher UTS and YS. Parts 2 and 4 were compared as they have the same orientation and volume. Also, the compact nature of the part geometry developed for this work allows for excellent isolation of the location variable and an accurate assessment of any effect of this variable on microstructure and mechanical properties. Although results (Table II) suggest the exterior part did have finer  $\alpha$  laths, UTS (1 % change), YS (2 % change), and microhardness were all lower than for the interior part. There was no observed difference in % EL or prior- $\beta$  grain size (Figure 4).

*Table II. Properties of horizontal location parts. A large change in location resulted in a small change in UTS (1 % change) and YS (2 % change).*

<b>part</b>	<b>description</b>	<b>UTS (MPa)</b>	<b>YS (MPa)</b>	<b>% EL</b>	<b><math>\alpha</math> lath thickness (<math>\mu\text{m}</math>)</b>	<b>microhardness (HV)</b>
2	interior	1029.7±7.0	982.9±5.7	12.2±0.8	0.95±0.31	372.0±7.2
4	exterior	1017.4±4.9	966.5±5.3	12.2±2.0	0.91±0.24	360.1±8.1
ANOVA	p-value	0.0003	<0.0001	>0.9999	0.02	<0.0001

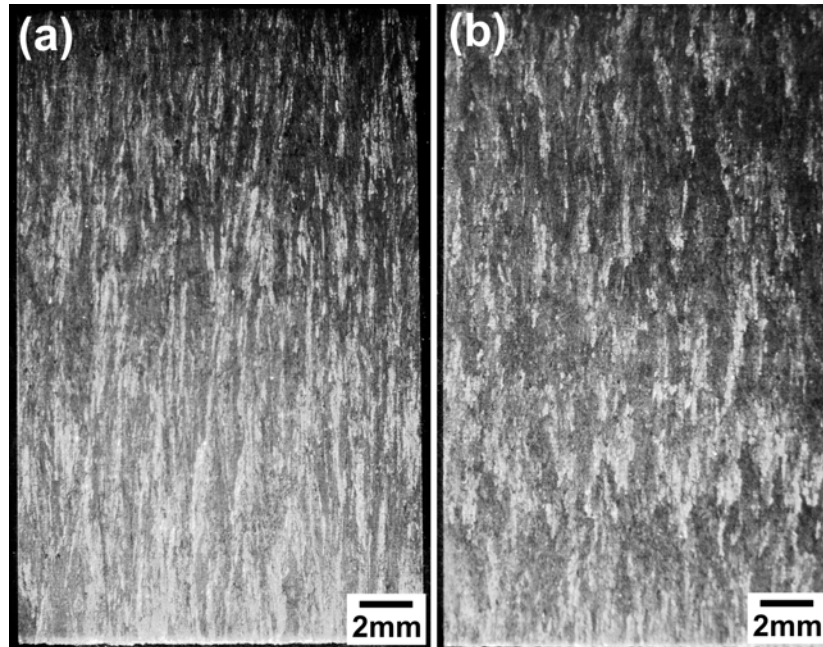


Figure 4. Macroscopic optical microscope images of (a) interior part 2 and (b) exterior part 4 showing prior- $\beta$  grain structure. The bottom of each image corresponds to the bottom of the part, adjacent to the build plate. The top of each image corresponds to the top of the part. The gradient of brightness is only due to the low-angle light used to capture the image and should not be mistaken as a microstructural feature. It appears there is little difference in grain size.

#### Location – vertical

Vertically oriented parts isolate the location variable even better than horizontal parts in the x-y plane, so interior part 3 and exterior part 5 were compared to investigate any trends. The same relationship between location and microstructure/mechanical properties was expected, but UTS (2 % change) and YS (2 % change) were again lower for the exterior part compared to the interior part (Table III). No differences in % EL,  $\alpha$  lath thickness, microhardness, or prior- $\beta$  grain size (Figure 5) were observed. Voids were observed on the fracture surfaces of 7 out of 10 tensile specimens for part 5 (Figure 6), compared to only 2 out of 10 tensile specimens for part 3. These voids were not observed on any of the horizontally built parts. In the x-y plane voids ranged in size (approximate minimum 150  $\mu\text{m}$ ) but were larger than the internal pores (approximate maximum 100  $\mu\text{m}$ , Figure 6a,b,c) that originate from hollow gas-atomized powder and remain in as-built material [11]. In the z-direction voids were relatively thin (approximate maximum 20  $\mu\text{m}$ , Figure 6d,e). Voids were also non-spherical compared to spherical internal pores. For all voids, unidirectional lines with the same orientation (left to right in Figure 6a) were observed. From observing the microstructure piece for part 5 (Figure 6d,e) voids occurred over a range of distances from the build plate, and seemed, qualitatively to decrease in number from the left side to the right side. There were no voids observed on the microstructure piece of part 3, so the trend observed in part 5 could not be verified.

Table III. Properties of vertical location parts. A large change in location resulted in a small change in UTS (2 % change) and YS (2 % change).

part	description	UTS (MPa)	YS (MPa)	% EL	$\alpha$ lath thickness ( $\mu\text{m}$ )	microhardness (HV)
3	interior	1032.9 $\pm$ 12.9	984.1 $\pm$ 8.5	9.0 $\pm$ 2.9	0.96 $\pm$ 0.26	367.6 $\pm$ 8.3
5	exterior	1008.6 $\pm$ 15.2	961.0 $\pm$ 7.1	7.1 $\pm$ 3.4	0.96 $\pm$ 0.27	368.4 $\pm$ 5.8
ANOVA	p-value	0.0013	<0.0001	0.2	>0.9999	0.69

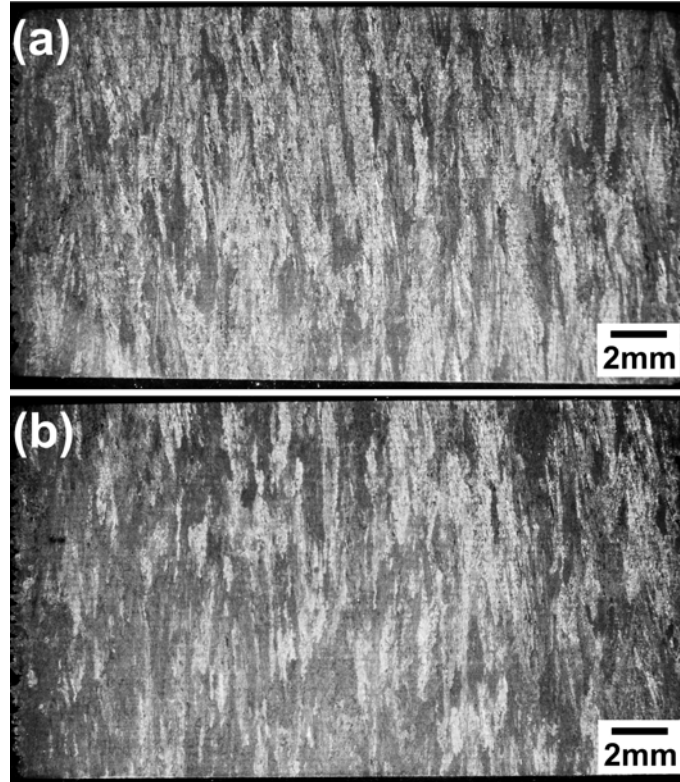


Figure 5. Macroscopic optical microscope images of (a) interior part 3 and (b) exterior part 5 showing prior- $\beta$  grain structure. The left edge shown in each image corresponds to the left edge of each part, and the right shown in each image corresponds to the right edge of each part. The gradient of brightness is only due to the low-angle light used to capture the image and should not be mistaken as a microstructural feature. It appears there is little difference in grain size.

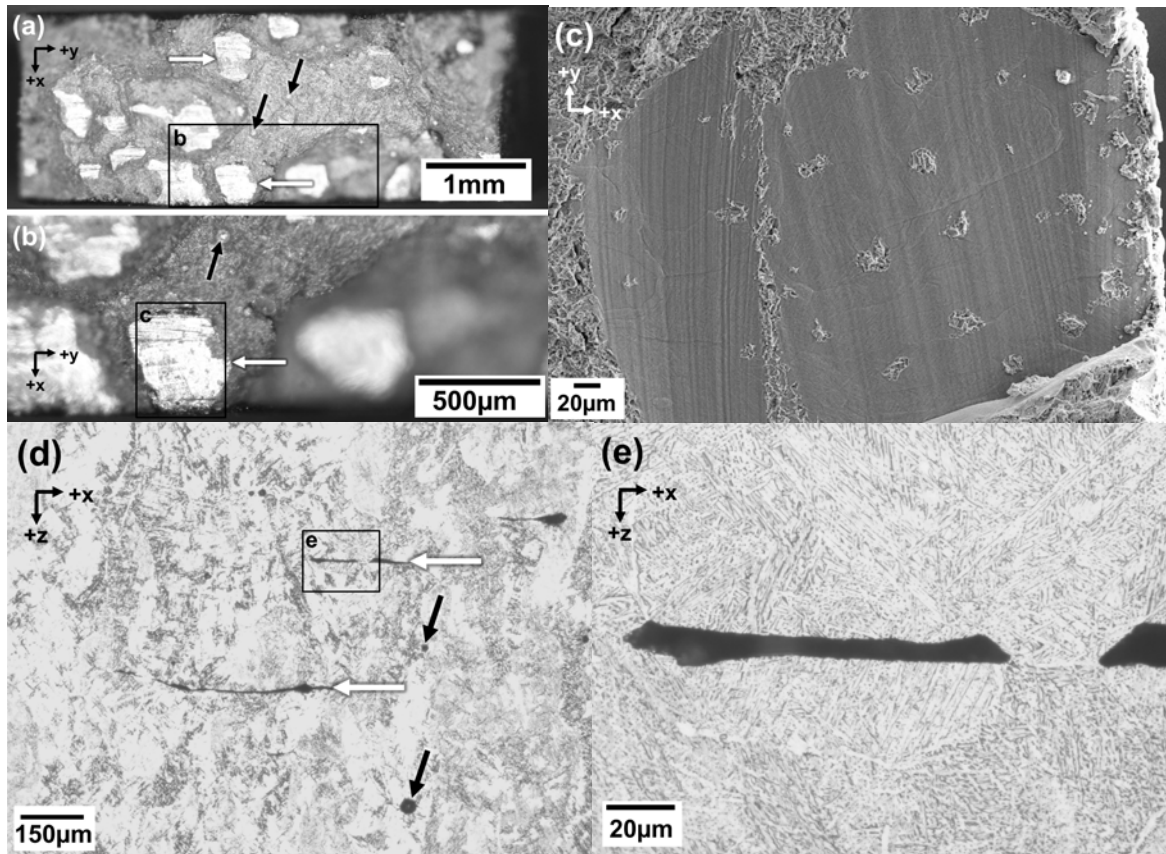


Figure 6. (a) and (b) optical microscope images (c) SEM image of part 5 tensile specimen fracture surface with 2.6 % EL showing top view of voids (black arrows) and internal pores (white arrows) (d) and (e) optical microscope images of EBM Ti-6Al-4V part 5 microstructure after etching showing side view of voids (black arrows) and internal pores (white arrows). Unidirectional lines were observed in the same orientation on all voids (left to right on (a) and (b)).

### Orientation – horizontal vs. vertical

The z-oriented texture in EBM Ti-6Al-4V [2] suggested microstructure and mechanical properties might change depending on part orientation. Horizontal part 2 and vertical part 3 were compared because the orientation of their tensile axes to texture direction differed. The influence of location was minimized as the parts were adjacent to each other, and both parts were the same volume. % EL was found to be considerably lower (30 % change) for the vertical part compared to the horizontal part (Table IV). Microhardness was also found to be lower for the vertical part despite no observable difference in UTS or YS. There was also no observable difference in  $\alpha$  lath thickness or prior- $\beta$  grain size (Figure 7). It is also important to point out that the prior- $\beta$  grain morphology of these parts is elongated in the z-direction as expected from previous EBM Ti-6Al-4V literature [2].

Table IV. Properties for horizontal vs. vertical orientation parts. Vertical part had 30% lower %EL. No difference was observed for UTS or YS.

part	description	UTS (MPa)	YS (MPa)	% EL	$\alpha$ lath thickness ( $\mu\text{m}$ )	microhardness (HV)
2	horizontal	1029.7 $\pm$ 7.0	982.9 $\pm$ 5.7	12.2 $\pm$ 0.8	0.95 $\pm$ 0.31	372.0 $\pm$ 7.2
3	vertical	1032.9 $\pm$ 12.9	984.1 $\pm$ 8.5	9.0 $\pm$ 2.9	0.96 $\pm$ 0.26	367.6 $\pm$ 8.3
ANOVA	p-value	0.5	0.72	0.01	0.65	0.02

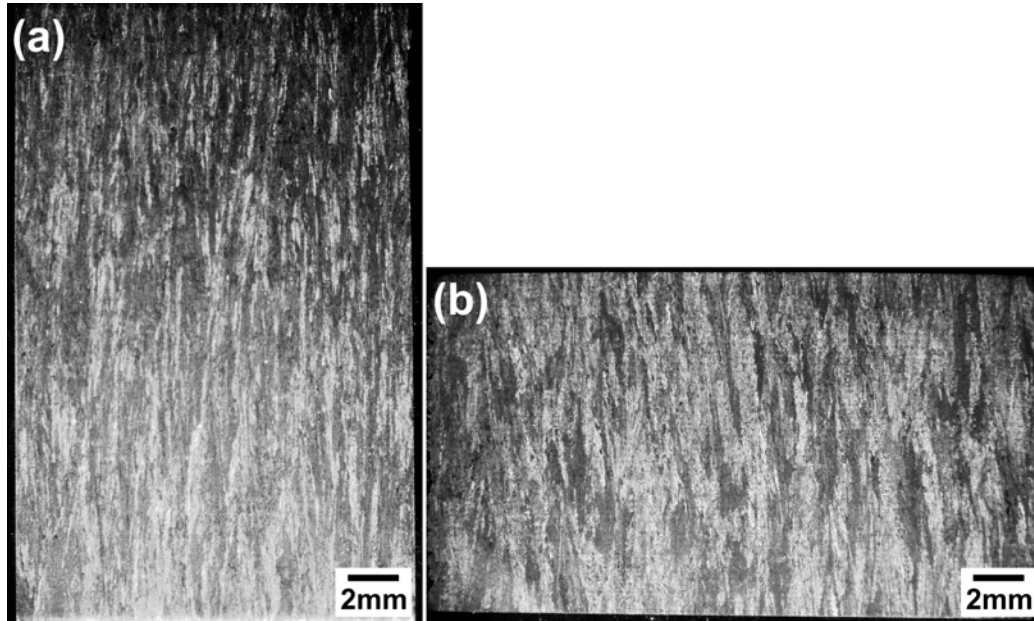


Figure 7. Macroscopic optical microscope images of (a) horizontal part 2 (bottom of image corresponds to the bottom of the part, adjacent to the build plate; top of image corresponds to the top of the part) and (b) vertical part 3 (left edge in image corresponds to the left edge of part; right edge in image corresponds to the right edge of part) showing prior- $\beta$  grain structure. The gradient of brightness is only due to the low-angle light used to capture the image and should not be mistaken as a microstructural feature. It appears there is little difference in grain size.

### Orientation – x vs. y

It was desirable to compare two parts of different orientation but with the same relationship between tensile axes and texture direction. X-oriented part 4 and y-oriented part 6 meet these criteria and although they are not adjacent, they are both on the edge of the build space. The hypothesized location effect would scale with distance from the center of the build space and be measured radially outward to the exterior of the build space. Therefore, any location effects were still minimized with these two parts as they were both at the exterior of the build space. The y-oriented part has a higher UTS (2 % change), YS (3 % change), and microhardness and a smaller  $\alpha$  lath thickness (Table V). There was no observable difference in % EL, but it appeared prior- $\beta$  grain size was smaller for the y-oriented part (Figure 8).

Table V. Properties for y vs. x orientation parts. A small change in UTS (2 % change) and YS (3 % change) was observed.

part	description	UTS (MPa)	YS (MPa)	%EL	$\alpha$ lath thickness ( $\mu\text{m}$ )	microhardness (HV)
4	x-oriented	1017.4 $\pm$ 4.9	966.5 $\pm$ 5.3	12.2 $\pm$ 2.0	0.91 $\pm$ 0.24	360.1 $\pm$ 8.1
6	y-oriented	1036.3 $\pm$ 4.8	993.1 $\pm$ 6.5	11.1 $\pm$ 2.2	0.80 $\pm$ 0.24	368.1 $\pm$ 7.0
ANOVA	p-value	<0.0001	<0.0001	0.26	<0.0001	<0.0001

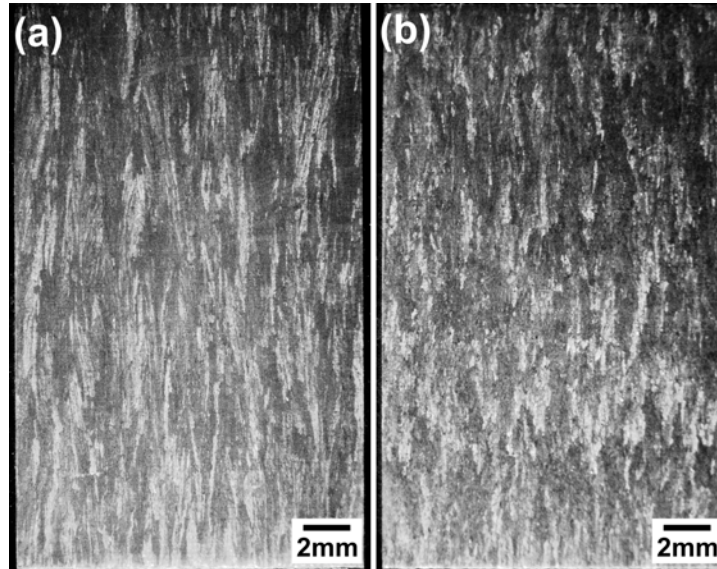


Figure 8. Macroscopic optical microscope images of (a) x-oriented part 4 and (b) y-oriented part 6 showing prior- $\beta$  grain structure. The bottom of each image corresponds to the bottom of the part, adjacent to the build plate. The top of each image corresponds to the top of the part. The gradient of brightness is only due to the low-angle light used to capture the image and should not be mistaken as a microstructural feature. It appears the y-oriented part has a smaller prior- $\beta$  grain size.

## DISCUSSION

### Location – horizontal

The magnitude of change in UTS (1 % change) and YS (2 % change) was relatively small despite a large difference in location (Table II). Compared to the interior part, the exterior part had lower UTS, YS, and microhardness as well as a smaller  $\alpha$  lath thickness. These relationships do not follow the known relationships between  $\alpha$  lath thickness and mechanical properties for the acicular Ti-6Al-4V microstructure [3-9]. One possible explanation is that the relationship between  $\alpha$  lath thickness and mechanical properties is different for EBM processed Ti-6AL-4V because its microstructure differs slightly from the expected acicular or Widmanstätten microstructure through classic annealing. This microstructure difference is explained in more detail in part 1 of this publication. The macroscopic images of prior- $\beta$  grain size (Figure 4) facilitate only qualitative assessment and may not be an appropriate method for distinguishing small differences in grain size. The mechanical property results are considered more trustworthy and will be used to identify any trends.

It was hypothesized that UTS and YS would be higher for the exterior part due to lower heat and faster cooling rates from beam deflection. However, the opposite trend was observed (Table II). It is possible that the small change in UTS and YS made it impossible to accurately determine any trends. If it is assumed the trend in the data is accurate, the second order effect of thermal mass might explain the results. The 1 mm spacing between adjacent parts was assumed to thermally isolate parts, but it is possible adjacent parts added heat and slowed cooling rates, leading to coarser microstructure and lower UTS and YS than expected. The exterior part (#4, Figure 1) in this case was part of a larger thermal mass (including the two parts “not characterized”) compared to that of the interior part (#2 and #1).

### **Location – vertical**

Similar to horizontally built location parts, for vertical location parts a large difference in location resulted in a small change in UTS (2 %) and YS (2 %) (Table III). The trend observed for the vertical location parts was opposite of the expected trend, but it is quite possible the small difference in UTS and YS makes accurate identification of any trends impossible. If the trend is assumed to be accurate, the second order effect of thermal mass does not help in this case because the interior part 3 had a higher thermal mass than the exterior part. The higher frequency of voids found in the exterior part (Figure 6) may have resulted in the observed UTS and YS trends. Out of spec oxygen content (Table I) and/or presence of large voids (Figure 6) could possibly have resulted in % EL for both parts failing to meet the requirement in ASTM F2924 (10 % minimum). If only tensile specimens without voids are considered, % EL for both parts meet ASTM F2924 requirements (10.2 %  $\pm$  1.6 % for part 3, 11.1 %  $\pm$  0.8 % for part 5). It is well documented for electron beam cold hearth melting (EBCHM) that aluminum vaporizes during melting of Ti-6Al-4V [15, 16]. This occurs for additive manufacturing EBM as well, leading to aluminum condensing and solidifying on parts of the build chamber such as the heat shields. Although the exact mechanism of void formation is unclear, the morphology of the voids leads us to hypothesize that aluminum-rich flakes are flaking off the heat shields and falling into the powder bed where they contribute to the formation of the observed voids.

### **Orientation – horizontal vs. vertical**

Horizontally built part 2 had a significantly larger % EL (30 % change) compared to the vertically built part 3, and no difference was found for UTS or YS (Table IV). The difference in % EL is attributed to differences in tensile axis orientation with respect to direction of elongated prior- $\beta$  grains and microstructural texture [2]. These results agree well with classically annealed bulk Ti-6Al-4V [5, 6] and one of the similar previous studies on EBM Ti-6Al-4V [10]. Unfortunately, there was insufficient methodology and part layout information provided in the other similar previous study [11] to speculate on any reasons for the difference in % EL trend observed.

### **Orientation – y vs. x**

Results for these parts (Table V) showed no difference in % EL, but there was a small difference in UTS (2 % change), YS (3 % change), microhardness,  $\alpha$  lath thickness, and prior- $\beta$  grain size. Orientation was not expected to have an effect in the x-y plane as the tensile axes for parts oriented in both directions were orthogonal to the texture direction [2]. It is possible the second order effect of thermal mass resulted in the observed differences. X-oriented part 4 was

adjacent to larger parts (“not characterized”, Figure 1) which could have slowed the cooling rate, leading to the observed coarser  $\alpha$  laths and prior- $\beta$  grain and lower UTS and YS compared to the more thermally isolated x-oriented part 6.

## CONCLUSIONS

Vertically oriented parts were found to have a considerably lower % EL (30 % change) compared to horizontally oriented parts, which was attributed to differences in tensile axis orientation in relation to the direction of elongated prior- $\beta$  grains and microstructural texture for EBM Ti-6Al-4V, and no difference in UTS or YS was observed. Orientation within the x-y plane and location were both found to have less than 3 % effects on mechanical properties, and a second order effect of thermal mass may have influenced these results. This study provides a framework for identifying and evaluating intra-build variations using a unique part geometry which allows for more accurate determination of influence from various processing variables. Variables should be evaluated for each new material, machine, and technique (e.g. EBM powder bed different from EBM wire feed) as part of a quality control process.

## ACKNOWLEDGMENTS

This research was performed while the author held a National Research Council Research Associateship Award at the National Institute of Standards and Technology.

## FOOTNOTES

<sup>1</sup>Commercial names are identified in order to specify the experimental procedure adequately. Such identification is not intended to imply recommendation or endorsement by the NIST nor does it imply that they are necessarily the best available for the purpose.

## REFERENCES

1. Svensson, M. and U. Ackelid. *Influence of Interstitial Elements on the Mechanical Properties of Ti-6Al-4V Produced with Electron Beam Melting*. in *Materials Science and Technology Conference*. 2011. Columbus, OH.
2. Al-Bermani, S.S., et al., *The Origin of Microstructural Diversity, Texture, and Mechanical Properties in Electron Beam Melted Ti-6Al-4V*. *Metallurgical and Materials Transactions A*, 2010. **41A**: p. 3422-3434.
3. Collings, E.W., *The Physical Metallurgy of Titanium Alloys*. 1984, Metals Park, OH: American Society for Metals.
4. Donachie, M.J., *Titanium: A Technical Guide*. 2nd ed. 1989, Metals Park, Ohio: ASM International.
5. Lütjering, G., J. Albrecht, and O.M. Ivasishin. *Influence of Cooling Rate and  $\beta$  Grain Size on the Tensile Properties of ( $\alpha$ + $\beta$ ) Ti Alloys*. in *8th World Titanium Conference Proceedings*. 1995.
6. Lütjering, G. and J.C. Williams, *Titanium*. 2nd ed. 2007, Berlin: Springer.
7. Rack, H.J. and J.I. Qazi, *Titanium Alloys for Biomedical Applications*. *Materials Science and Engineering C*, 2006. **26**: p. 1269-1277.

8. Tiley, J., et al., *Quantification of Microstructural Features in  $\alpha/\beta$  titanium alloys*. Materials Science and Engineering A, 2004. **372**: p. 191-198.
9. Welsch, G., R. Boyer, and E.W. Collings, *Materials Properties Handbook: Titanium Alloys*. 1994, Metals Park, OH: ASM International.
10. Bass, B.S., *Validating the Arcam EBM Process as an Alternative Fabrication Method for Titanium-6Al-4V Alloys*, in *Materials Science and Engineering*. 2007, M.S. Thesis, North Carolina State University Raleigh, NC. p. 57.
11. Ackelid, U. and M. Svensson. *Additive Manufacturing of Dense Metal Parts by Electron Beam Melting*. in *Materials Science and Technology Conference*. 2009. Pittsburgh, PA: MS&T Partner Societies.
12. Lach, C. and R.A. Hafley. *Fractographic Characterization of Electron Beam Freeform Fabrication Produced Ti-6Al-4V*. in *TMS Conference*. 2012. Orlando, FL.
13. Hrabe, N., R. Kircher, and T. Quinn, *Effects of Processing on Microstructure and Mechanical Properties of Ti-6Al-4V Fabricated using Electron Beam Melting (EBM), Part 1: Distance from Build Plate and Part Size*. Materials Science and Engineering A, 2012. **submitted**.
14. Schneider, C.A., W.S. Rasband, and K.W. Eliceiri, *NIH Image to ImageJ: 25years of image analysis*. Nature Methods, 2012. **9**: p. 671-675.
15. Ivanchenko, V.G., O.M. Ivasishin, and S.L. Semiatin, *Evaluation of Evaporation Losses during Electron-Beam Melting of Ti-Al-V Alloys*. Metallurgical and Materials Transactions B, 2003. **34B**(December): p. 911-915.
16. Semiatin, S.L., et al., *Diffusion Models for Evaporation Losses during Electron-Beam Melting of Alpha/Beta-Titanium Alloys*. Metallurgical and Materials Transactions B, 2004. **35B**(April): p. 235-245.